Scale-Free Antiferromagnetic Fluctuations in the $s = 1/2$ Kagome Antiferromagnet Herbertsmithite

M. A. de Vries,[1,2,3,*] J. R. Stewart,[4,5] P. P. Deen,[4] J. O. Piatek,[2] G. J. Nilsen,[2] H. M. Rønnow,[2] and A. Harrison[4,3]

[1]*School of Physics & Astronomy, University of St-Andrews, the North Haugh, St Andrews, KY16 9SS, United Kingdom*
[2]*Laboratory for Quantum Magnetism, École Polytechnique Fédérale de Lausanne (EPFL), Switzerland*
[3]*CSEC and School of Chemistry, The University of Edinburgh, Edinburgh, EH9 3JZ, United Kingdom*
[4]*Institut Laue-Langevin, 6 rue Jules Horowitz, F-38042 Grenoble, France*
[5]*ISIS facility, Rutherford Appleton Laboratories, STFC, Chilton, Didcot OX11 0DE, United Kingdom*

(Received 18 February 2009; revised manuscript received 12 October 2009; published 2 December 2009)

Neutron spectroscopy and diffuse neutron scattering on herbertsmithite [$ZnCu_3(OH)_6Cl_2$], a near-ideal realization of the $s = 1/2$ kagome antiferromagnet, reveal the hallmark property of a quantum spin liquid: instantaneous short-ranged antiferromagnetic correlations in the absence of a time-averaged ordered moment. These dynamic antiferromagnetic correlations are weakly dependent of neutron-energy transfer and temperature, and persist up to 25 meV and 120 K. At low energy transfers a shift of the magnetic scattering to low Q is observed with increasing temperature, providing evidence of gapless spinons. It is argued that these observations provide important evidence in favor of resonating-valence-bond theories of (doped) Mott insulators.

DOI: 10.1103/PhysRevLett.103.237201 PACS numbers: 75.40.Gb, 74.40.+k, 75.45.+j

There has been a long search for quantum spin liquids in Mott insulators in which the common Néel antiferromagnetic order is destabilized by quantum fluctuations [1,2], the mixing-in of spin singlets. The $s = 1/2$ kagome antiferromagnet is one system where such a spin liquid state could, in theory, be found. The kagome lattice, which owes its name to a Japanese basket weaving method, is a net of corner-sharing triangles. When antiferromagnetically-coupled spins are arranged at the vertices of this lattice it becomes impossible to satisfy all antiferromagnetic (AF) bonds simultaneously. Because of this geometric frustration, the ground state has a continuous and macroscopic degeneracy.

Both in the classical limit of large spin [3,4] and in the quantum limit of $s = 1/2$ [5], the kagome antiferromagnet has been predicted to retain the full symmetry of the magnetic Hamiltonian. Exact diagonalization (ED) results suggest that in the macroscopic limit of the $s = 1/2$ system a continuum of nonmagnetic global spin-singlet $s_{\mathrm{tot}} = 0$ states fills an energy gap to magnetic excitations [6]. Whether there is a spin gap in real systems has however been debated and in most theories building on Anderson's resonating-valence-bond proposal [2], such as the algebraic spin liquid (ASL) [7–9], there are gapless spinons [7,10]. Spinons are $s = 1/2$ excitations which are created in pairs following a singlet-triplet excitation but can dissociate with no (additional) cost in energy. The ASL is thought of as a ''mother of competing orders'' [11] including Néel antiferromagnetism and d-wave superconductivity. As the insulating analogue for the Fermi liquid in metals the ASL would be a natural candidate for the ground state in a Mott insulator where Néel order is suppressed. The results presented here on the kagome AF compound herbertsmithite provide further evidence for this idea. At the same time, the absence of a spin gap in herbertsmithite can be reconciled with ED results [12] when a Dzyaloshinky-Moriya interaction [13] or structural disorder is taken into account.

Of the many kagome systems studied experimentally, including the jarosites [14,15], SCGO ($SrCr_{8-x}Ga_{4+x}O_{19}$) [16] and volborthite [17], herbertsmithite [$ZnCu_3(OH)_6Cl_2$] [18] is the first where no (partial) freezing of the spins is observed down to the lowest temperatures accessible experimentally [19,20]. The Weiss temperature is 300 K and the AF exchange interaction $J \approx 190$ K [6,20]. Herbertsmithite contains well separated 2D kagome layers of Cu^{2+} ions linked by O^{2-} ions in OH^- groups. Separating the kagome layers are Zn sites of O_h symmetry, which can also host Cu^{2+} ions to form the zinc paratacamite family $Zn_xCu_{4-x}(OH)_6Cl_2$ with $0 < x \leq 1$. For $x = 1$ the low-temperature susceptibility is dominated by a Curie-like contribution from ''antisite spins'' (a $\sim$6% fraction of Cu^{2+} spins which have traded places with Zn^{2+} to occupy the interplane Zn site) [21,22]. These weakly-coupled $s = 1/2$ spins, which have been identified as individual doublets [21], have also been observed in neutron spectra at the Zeeman energy in applied fields [20,23]. Using ^{17}O NMR [24] and Cl NMR [25] there is now convincing evidence that the kagome layers have a nonzero susceptibility as $T \to 0$. This is in agreement with the continuum of magnetic excitations observed using neutron spectroscopy at energies between $\sim$0.8 and 2 meV [20]. Moreover, this spectrum is independent of the temperature, which has been suggested to point to the proximity of a quantum critical point [20]. Here we present neutron spectroscopy data up to energy transfers of $\sim$30 meV and

temperatures up to 120 K, to measure the dynamic magnetic structure factor and fully characterize the quantum spin dynamics in herbertsmithite.

Large single crystals of herbertsmithite do not presently exist. Hence, 20 g of 98% deuterated herbertsmithite powder was synthesized following the method as described in Ref. [18]. This sample was characterized using neutron diffraction, dc magnetic susceptibility, heat capacity [21] and μSR measurements [19]. The measurements were carried out using the polarized neutron spectrometers $D7$ and IN22, and the time-of-flight (TOF) spectrometers IN4, ILL, France, and MARI, ISIS, UK. At $D7$ the magnetic scattering was separated from the nuclear and spin-incoherent scattered neutrons using XYZ polarization analysis [26]. No energy analysis was carried out on the scattered neutrons, with an incident neutron energy of 8.95 meV, effectively energy integrating the neutron cross section [27] up to energy transfers (ϵ) of $\sim$6.5 meV. Complete $S(Q, \epsilon)$ maps without polarization analysis were obtained at 2, 4, 10, 30, 60, and 120 K at IN4 using 17.21 meV neutrons and at 2 K at MARI using 56 meV neutrons. The normalized spin and nuclear incoherent signals measured at $D7$ were used to normalize the IN4 and MARI data. Neutron polarization and energy resolved measurements were carried out at the triple-axis spectrometer IN22, ILL. Several Q, ϵ and T scans were performed for spin flip (SF) and non-spin flip (NSF) channels for incident and scattered neutron spins polarized parallel to Q (labeled xx) and perpendicular to Q (labeled zz).

At $D7$ the energy of the scattered neutrons is not analyzed. The $D7$ data [Fig. 1(a)] therefore correspond to magnetic correlations which persist on a time scale of at most [27] $\sim$6.5 meV (1.6 THz). The broad peak observed here at 1.3 Å^{-1} is direct evidence of short-ranged instantaneous near-neighbor AF correlations. For comparison, the powder-averaged structure factor for uncorrelated near-neighbor AF dimers given by

$$F^2(Q)\left(1 - \frac{\sin(Qd)}{Qd}\right), \tag{1}$$

is shown in Figs. 1(a) and 1(b). In Eq. (1) $F(Q)$ is the Cu^{2+} magnetic form factor and $d = a/2 = 3.42$ Å the Cu-Cu distance within the kagome plane.

Similar short-ranged AF correlations are observed in the TOF data from IN4 and MARI at all ϵ accessed, up to 25 meV. Figures 1(b) and 1(c) show, respectively, the momentum and energy dependence of the magnetic scattering peak in the TOF data. Figure 2 shows scans in ϵ, temperature, and Q using polarization analysis which confirm that these dynamic correlations are of magnetic origin. That a similar Q dependence is observed in the $D7$ data suggests that the dynamic magnetic correlations remain unchanged down to the elastic line. From Figs. 2(b)–2(d) it is clear that in addition to magnetic inelastic scattering (S_{mag}) there is significant inelastic background from spin-incoherent ($\mathrm{SF_{inc}} = \mathrm{SF}_{zz} - S_{\mathrm{mag}}$) and nuclear scattering. This is ascribed to incoherent scattering from residual protons and multiple scattering. This background is also present in the IN4 data and to a lesser extent in the MARI data because there a smaller sample was mounted in an annular geometry. The integrated intensity of the dynamic AF correlations as found in Figs. 1 and 2 up to 25 meV

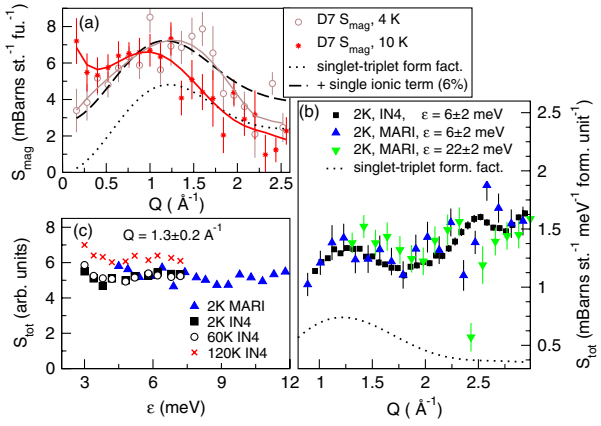

FIG. 1 (color online). (a) Instantaneous magnetic correlations at 4 K (open circles) and 10 K (filled circles) from $D7$. Data taken at 60 K (not shown) resemble the 10 K data. The solid lines are a guide to the eye. (b) The Q dependence in the dynamic correlations from IN4 and MARI with the energy integration interval indicated in the legend. The dotted line in panel (a) and (b) is the structure factor for dimerlike AF correlations, for the dashed line a single-ion contribution corresponding to the 6% antisite spins in this system is added. (c) The energy and temperature dependence at $Q = 1.3$ Å^{-1} from the TOF data.

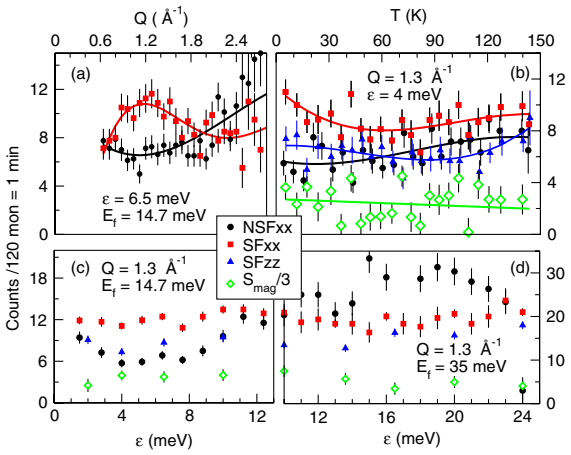

FIG. 2 (color online). Inelastic intensity for 3 polarization channels: NSF_{xx} contains phonons and NSF background. SF_{xx} contains 2/3 of the magnetic intensity and SF background. SF_{zz} contains 1/3 of the magnetic intensity. Hence, $S_{\mathrm{mag}}/3 = \mathrm{SF}_{xx} - \mathrm{SF}_{zz}$. It is seen that magnetic intensity at the maximum at $Q = 1.3$ Å^{-1} [SF_{xx} in panel (a)] is finite and nearly constant for all covered temperatures (b) and energies (c),(d). Data in (a), (c), and (d) were measured at 2 K.

corresponds to 30% to 50% of the sum rule $s(s+1)$ for the spins on the kagome lattice.

In the raw IN4 data the dynamic correlations at $Q < 1.8$ Å^{-1} persist up to 30 K while the magnetic scattering at the maximum of the peak at 1.3 Å^{-1} changes very little up to 120 K [Figs. 1(c) and 2(b)]. The intensity at the energy loss side ($\epsilon < 0$) in the TOF data obeys detailed balance at all temperatures. This combined with the magnetic scattering intensity and temperature dependence in the $D7$ data implies that at the elastic line there must be increased magnetic scattering, but still with the same Q dependence. These (quasi) static magnetic correlations are reduced with a shift of intensity to lower Q as the temperature is increased, in what looks like spinon excitations in the $D7$ data at 10 K [Fig. 1(a)].

The above observations complement previous neutron spectroscopy results on herbertsmithite [20], which show the inelastic magnetic scattering cross section is energy independent between 0.8 and 2 meV apart from a weak field-dependent peak which is due to the weakly-coupled Cu^{2+} spins on Zn sites. The Q dependence in this energy range is not peaked at 1.3 Å^{-1} which is due to the single ion contribution from antisite spins. This contribution also needs to be added to Eq. (1) to fit the $D7$ data. The absence of a peak around the edge of the first Brillouin zone in Ref. [20] down to 35 mK implies there is no significant increase of the dynamic magnetic correlations over 3 orders of magnitude in temperature.

At $Q > 1.8$ Å^{-1} and for $T > 30$ K the inelastic scattering is increasingly dominated by phonons. The temperature dependence of phonon scattering can in general be calculated from a temperature independent dynamic susceptibility using the fluctuation dissipation theorem. The temperature independence of the magnetic scattering observed at low Q prompted us to fit the temperature dependence of each pixel in $S(Q, \epsilon; T)$ [Figs. 3(a) and 3(b) for $T = 2$ K and 120 K, respectively] as the sum of a temperature independent component $S_{\mathrm{AF}}(Q, \epsilon)$ and a component following linear response $\chi''(Q, \epsilon)$,

$$S(Q, \epsilon; T) = S_{\mathrm{AF}}(Q, \epsilon) + (1 - e^{-\epsilon/k_B T})^{-1} \chi''(Q, \epsilon). \quad (2)$$

The $S_{\mathrm{AF}}(Q, \epsilon)$ and $\chi''(Q, \epsilon)$ resulting from the fit are shown in Figs. 3(c) and 3(d), respectively. As expected, $S_{\mathrm{AF}}(Q, \epsilon)$ corresponds to the raw data from IN4 at low Q and $T < 60$ K and there is a good overall agreement with the structure factor of Eq. (1) [Fig. 4(a)] added to a constant background. Phonon dispersion originating from the nuclear Bragg peaks is on the other hand clearly visible in $\chi''(Q, \epsilon)$. The excellent fit for all data at 6 different temperatures, as illustrated in Fig. 4(b) for a small sample of points, confirms that the magnetic correlation length does not diverge as the temperature is lowered and that these dynamic correlations persist up to at least 120 K. The maximum in χ'' and $S(Q, \epsilon)$ around 7 meV that extends

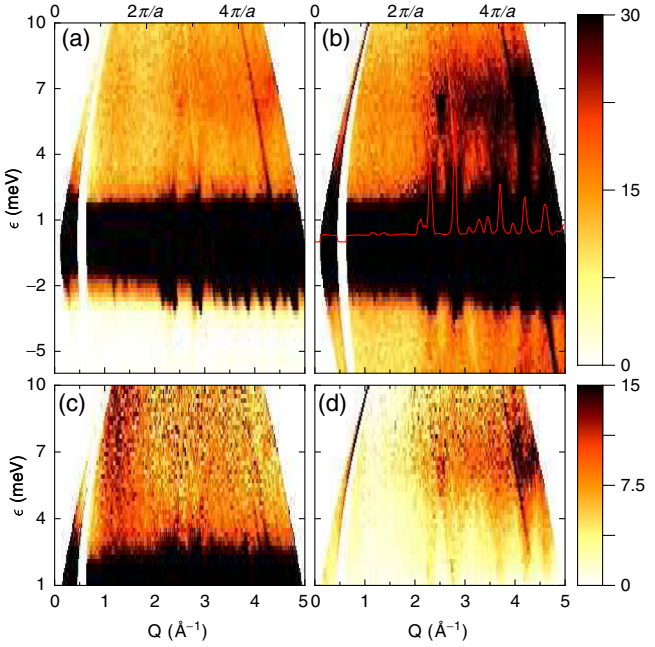

FIG. 3 (color online). The scattering cross section $S(Q, \epsilon)$ of at 2 K (a) and 120 K (b). The intensity scale is mb sr^{-1} meV^{-1} f.u.$^{-1}$. The elastic powder diffraction pattern is also shown in (b). Panel (c) and (d) show respectively S_{AF} and χ''. The white band at low Q is a gap between detectors. Some increase in intensity in S_{AF} is observed at higher energies but this is likely due to the direct beam and larger error bars. As shown in Fig. 4(a) the increase in intensity is only very small.

to $Q < 1.8$ Å^{-1} gives the impression of an increase in magnetic scattering at $(Q, \epsilon) = (1.3$ Å$^{-1}, 7$ meV). This signal in χ'' at low Q is most likely due to some weak multiple scattering at IN4 because it was not observed in the MARI and IN22 data.

Hence, we found that (1) At low frequencies ($\epsilon < 2$ meV) there is a shift of intensity to lower Q as the temperature increases, which could be due to (gapless) spinons. Spinons then also account for the nonzero magnetic susceptibility as measured with ^{17}O NMR [24]. (2) There

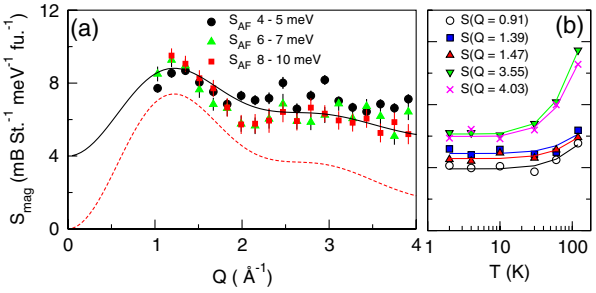

FIG. 4 (color online). (a) The Q dependence in $S_{\mathrm{AF}}(Q, \epsilon)$ for a number of energy transfers. (b) The temperature dependence for a number of points in $S(Q, \epsilon = 4$ meV) and fits to the data using Eq. (2).

are dynamic AF correlations with a very weak temperature and energy dependence, extending over more than 3 orders of magnitude in temperature and 2 orders of magnitude in energy. Hence, the dynamic AF correlations are approximately scale free. There is no characteristic energy scale in the system, not even one determined by temperature as in systems with ω/T scaling (with $\omega = \epsilon/\hbar$) and as expected for the ASL [9]. Although with neutron scattering any long range order of spin-singlet dimers cannot be detected directly, the absence of a spin gap and the temperature independent dynamic correlations observed here and in [20] imply the absence of a static dimerization, at least down to 35 mK. Short-ranged dynamic correlations are commonly observed in quantum spin liquids at temperatures well above their respective ordering and spin-glass transitions [16,28,29]. The temperature independence of the dynamic AF correlations observed here suggests that, intriguingly, the short-ranged dynamic correlations could be a property of the ground state in herbertsmithite.

A system of particular relevance in the present context is the spin-glass phase in $La_{2-x}Sr_xCuO_4$ (LSCO) with doping around $x = 0.05$ [30,31]. At this level of doping, just enough for the Néel order to be completely suppressed, the correlation length of the dynamic AF correlations becomes temperature independent not far below the Néel temperature of the parent compound. Such a strong likeness with the dynamic magnetic correlations in herbertsmithite is in agreement with resonating-valence-bond theories, which predict that the Mott insulator in the absence of Néel order and the pseudogap phases are closely related states. One proposal is that both are described by a staggered-flux, or algebraic spin liquid [7,9], a state with algebraically diverging correlations. Here the agreement with the spatial and temporal correlations in herbertsmithite, and with the spatial correlations in LSCO, breaks down. This could be due to weak structural disorder in the respective Cu-O planes which both systems are known to suffer from. To test this possibility new herbertsmithite samples are needed with reduced antisite disorder. The energy spectrum and powder-averaged Q dependence measured here are, apart from the absence of a spin gap, also in rough agreement with ED results [12] but large single crystals and theoretical predictions on the temperature dependence would be needed for a more detailed comparison.

L.-P. Regnault (CEA, Grenoble) is acknowledged for assistance with the IN22 measurements. We are also grateful for fruitful discussions with D. Ivanov and S. Bieri (EPFL), O. Cepas (Institut Néel, Grenoble), Jorge Quintanilla (ISIS, RAL), A. Huxley (Univeristy of Edinburgh), J. Zaanen (Leiden University) and J. Chalker (Oxford University). M. d. V. acknowledges an exchange grant from the HFM network of the European Science Foundation.

*m.a.devries@physics.org
Present address: School of Physics and Astronomy, University of Leeds, Leeds LS2 9JT, United Kingdom.

[1] G. Misguich and C. Lhuillier, in *Two-dimensional Quantum Antiferromagnets*, edited by H. T. Diep (World Scientific Publishing, Singapore, 2004), pp. 229–306.
[2] P. W. Anderson, Science **235**, 1196 (1987).
[3] J. N. Reimers, A. J. Berlinsky, and A.-C. Shi, Phys. Rev. B **43**, 865 (1991).
[4] I. Ritchey, P. Chandra, and P. Coleman, Phys. Rev. B **47**, 15 342 (1993).
[5] J. T. Chalker and J. F. G. Eastmond, Phys. Rev. B **46**, 14 201 (1992).
[6] G. Misguich and P. Sindzingre, Eur. Phys. J. B **59**, 305 (2007).
[7] I. Affleck and J. B. Marston, Phys. Rev. B **37**, 3774 (1988).
[8] Y. Ran, M. Hermele, P. A. Lee, and X.-G. Wen, Phys. Rev. Lett. **98**, 117205 (2007).
[9] M. Hermele, Y. Ran, P. A. Lee, and X.-G. Wen, Phys. Rev. B **77**, 224413 (2008).
[10] P. A. Lee, Rep. Prog. Phys. **71**, 012501 (2008).
[11] M. Hermele, T. Senthil, and M. P. A. Fisher, Phys. Rev. B **72**, 104404 (2005).
[12] A. Laeuchli and C. Lhuillier, arXiv:0901.1065.
[13] O. Cepas, C. M. Fong, P. W. Leung, and C. Lhuillier, Phys. Rev. B **78**, 140405(R) (2008).
[14] D. Grohol *et al.*, Nature Mater. **4**, 323 (2005).
[15] F. C. Coomer *et al.*, J. Phys. Condens. Matter **18**, 8847 (2006).
[16] C. Broholm, G. Aeppli, G. P. Espinosa, and A. S. Cooper, Phys. Rev. Lett. **65**, 3173 (1990).
[17] Z. Hiroi *et al.*, J. Phys. Soc. Jpn. **70**, 3377 (2001).
[18] M. P. Shores, E. A. Nytko, B. M. Bartlett, and D. G. Nocera, J. Am. Chem. Soc. **127**, 13 462 (2005).
[19] P. Mendels *et al.*, Phys. Rev. Lett. **98**, 077204 (2007).
[20] J. S. Helton *et al.*, Phys. Rev. Lett. **98**, 107204 (2007).
[21] M. A. de Vries, K. V. Kamenev, W. A. Kockelmann, J. Sanchez-Benitez, and A. Harrison, Phys. Rev. Lett. **100**, 157205 (2008).
[22] F. Bert *et al.*, Phys. Rev. B **76**, 132411 (2007).
[23] S.-H. Lee *et al.*, Nature Mater. **6**, 853 (2007).
[24] A. Olariu *et al.*, Phys. Rev. Lett. **100**, 087202 (2008).
[25] T. Imai, E. A. Nytko, B. M. Bartlett, M. P. Shores, and D. G. Nocera, Phys. Rev. Lett. **100**, 077203 (2008).
[26] J. R. Stewart *et al.*, J. Appl. Crystallogr. **42**, 69 (2008).
[27] The upper limit for the frequencies which are probed are a function of Q, approaching 0 as $Q \rightarrow 0$.
[28] W. Schweika, M. Valldor, and P. Lemmens, Phys. Rev. Lett. **98**, 067201 (2007).
[29] G. Shirane *et al.*, Phys. Rev. Lett. **59**, 1613 (1987).
[30] B. Keimer *et al.*, Phys. Rev. Lett. **67**, 1930 (1991).
[31] S. M. Hayden *et al.*, Phys. Rev. Lett. **66**, 821 (1991).